J. Mater. Environ. Sci. 7 (10) (2016) 3548-3557 *Bove et al.*
ISSN : 2028-2508
CODEN: JMESCN **CIAT2015**

Experimental and numerical analyses on the antiseismic effectiveness of fiber textile for earthen buildings

A. Bove, G. Misseri, L. Rovero*, U. Tonietti
Department of Architecture, University of Florence, Florence, Italy.

* *Corresponding author: L. Rovero, Tel: +39 055 2756846; E-mail address: luisa.rovero@unifi.it*

Abstract
Seismic risk represents one of major threats for earthen constructions. In case of earthquake, earthen buildings are exposed to horizontal forces, which induce tensile stresses not compatible with earthen materials, thus causing damage and collapse mechanisms. In last years, nets embedded in thin layers of earthen mortar on the external surface of walls have been proposed in order to strengthen the buildings against seismic actions. The effectiveness of such a system basically depends on the adhesion between net and earth and on the wall-net anchorage solution too. This paper presents the results of an experimental and a numerical analysis carried out in order to evaluate the effectiveness of retrofitting based on two types of natural fibers: jute and a coconut derivate. Experimental analysis comprised three-point bending tests on adobe bricks reinforced on the intrados with the natural fiber net. The experimental results were employed to carry out a numerical analysis through DIANA 9.6 with the goal of obtaining a numerical model useful to design retrofitting interventions

Keywords: reinforced adobe, natural fiber, seismic vulnerability, experimental testing, non-linear static FEM

1. Introduction
Earthen buildings host a great part of world population, representing one of the most spread constructive typologies in many countries, especially in rural areas. They are also a testimony of significant spontaneous architectural cultures, mostly related to a specific sustainable relationship with the environment, by which different modalities of settlement are characterized. A large part of these settlements is located in seismic prone areas, circumstance that strongly influences the safety of the inhabitants.
The earth material is less resistant than the stone or fired bricks (Houben, 2005; Islam et al., 2010; Omar Sidik et al., 2011; Baglioni et al., 2013; Gamrani et al., 2012; Fratini et al., 2011; Briccoli et al., 2008), but earthen buildings subjected to vertical loads (self and working weights) can exhibit a good stability as well the thick bearing walls ensure low compressive stresses (and they are protected from the weather). However, the same buildings show a great vulnerability if affected by seismic events. In case of earthquakes, a building is exposed to horizontal forces with alternating sign which induce both compressive and tensile stresses, thus causing damage and the collapse mechanisms. Sometimes local cultures were able to enhance the behavior of earthen buildings by improving construction techniques, but often the sparse occurrence of earthquakes (the so-called return period) and especially the poor economic conditions made these measures unfeasible. This is why the problem of defense against earthquakes is still an issue of great interest in many contexts.
In the tradition and in recent times, two main strategies are basically adopted in order to improve the behavior of earthen constructions; they consist in the improvement of the mechanical properties of material or of the global behavior of the structure. This second strategy is particularly appropriate to counteract the effects of earthquakes, and can be pursued by improving the resisting properties of the masonry wall box, retrofitting the connections among the walls (and among walls and stories) or by adopting strategies that increase ductility.
With this aim, many building cultures adopted the insertion of wooden structural elements (when available in the environment) or through tie-beams and story belts, as local devices, or creating a real infill-frame structure. This is the case of many building cultures from Balkan area up to Himalaya and, similarly along the whole

oceanic ridge of the Americas (Langhenbach, 2007; Omar Sidik et al., 2012). In recent years - together with the rediscovery of materials and technologies accessible and sustainable to improve the performance of buildings - the application of nets (plastic, metal or natural fibres) anchored and covered with mud mortar on the external walls surface have been proposed in order to strengthen the buildings against seismic actions (Minke, 2001; Blondet et al., 2003; Hardy et al., 2006; Blondet et al., 2007; Vargas et al., 2007; Torrealva et al., 2008; Méndez et al., 2008; Fischer, 2009; Méndez et al., 2010; Omar Sidik et al., 2012). Such a solution can be seen as the "poor" face of composite materials (Briccoli, 2008; Rovero et. Al., 2013; Rotunno et al., 2014), but it is certainly capable to play an important role since it, despite being innovative, does not need special technology or expensive tools. The effectiveness of such a system depends on the adhesion between net and earth and on the wall-net anchorage solution too.
This paper presents the results of experimental and numerical analyses carried out in order to evaluate the effectiveness of strengthening systems based on two types of natural fibers, jute and a coconut derivate. The results of the experimental investigation, already shown in (Omar Sidik et. al 2011) were used to develop and calibrate a numerical model capable of representing the adobe brick reinforced with natural nets. In particular, the experimental analysis comprised three-point bending tests on adobe bricks reinforced on the intrados with the textiles embedded on an earthen mortar layer. The three-point bending test has been proposed as an acceptance test for earthen materials, both in standard codes (Standards Australia Handbook 194, 2002; New Zealand Standard 4298, 1998) and in research works (Houben, 2005; Morel, 2002; Briccoli et al., 2008). In fact, it may be carried out rather easily directly on the bricks at the building site without the need for cuts or the need to create ad hoc specimens. The load which produces the collapse of adobe bricks by bending is very low and does not require the use of special presses (it is in fact possible to apply the load simply by overlaying bricks). Moreover, the bending test furnishes an evaluation of the compressive strength because for brittle material the compressive strength can be derived from the tensile strength (Morel, 2002; Briccoli et al., 2008).
The three-point bending tests permitted to evaluate the increase of tensile strength due to the net and to understand the behavior of the net-adobe interface.
On the base of the experimental results, a numerical model for the reinforced adobe was developed with the goal of obtaining a tool useful to design retrofitting interventions.
Taking into account the difficulties of an actual representation of the mechanical behavior for non-standard materials, non-linear analyses were carried out exploiting DIANA 9.6 code.
This research aims to contribute to an evaluation of strengthening techniques effectiveness in order to carry out adequate consolidation designs able to achieve a better seismic response for earthen structures. This objective is part of a general project indented to support safeguarding and rebuilding designs, using the experience acquired and validated in various constructive contexts (Rovero et al., 2009; Rovero and Fratini, 2013; Sani et al., 2012; Rovero and Tonietti, 2012; Fratini et al., 2011; Gamrat et al., 2012; Rovero and Tonietti, 2014).

2. The experimental analysis

2.1. Experimental set-up

The experimental analysis regarded three-point bending tests on adobe bricks in unreinforced and reinforced configuration, in order to evaluate the increase in strength and deformability produced by the net reinforcement placed at the intrados of the adobe (Figure 1).

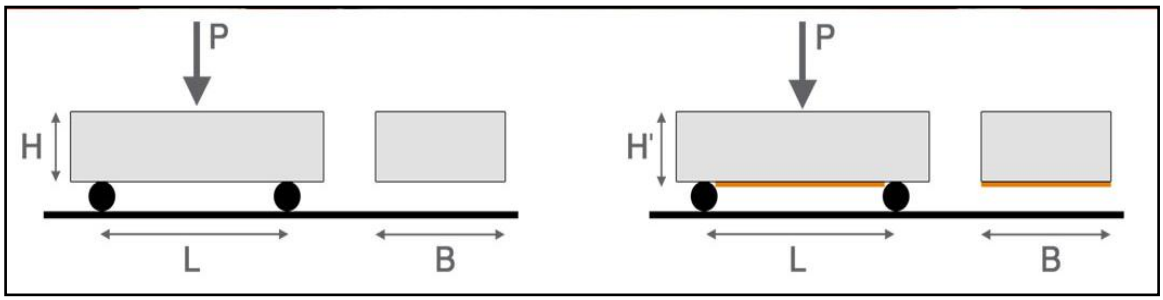

Figure 1: Sketch of the tree point test of unreinforced and reinforced adobe brick. H: unreinforced adobe brick thickness, H': reinforced adobe brick thickness, including textile and earthen matrix thickness, B: depth of the reinforcement (entire brick depth) and L: length of reinforcement (comprised between lower supports).

The test set-up is represented in Figure 2; a load cell (TCLP-5B Tokyo Sokki Kenkyujo Co. Ltd) with a capacity of 5 kN is connected to the screw jack (MTP7010 un-imec), and two displacement transducers (CE-10) were used to measure vertical displacements of the middle cross section of the adobe brick. The tests were conducted in displacement control in order to recorder the load-displacement diagram also after the peak load. The data acquisition was made through an electronic acquisition unit (NI cDAQ-9178 National Instruments) and the data logging software Lab-View Signal Express 2012.

Figure 2: Experimental set-up.

2.2. Specimens

Wood formworks were used for the realization of the fifteen specimens, sized 420x210x105 mm after a 5% of shrinkage.

The two kinds of net, respectively made of coconut or jute fibers, were kindly supplied by HARPO Spa (Trieste, IT). The Geojuta® and Coconet® products are intended for geotechnical consolidation purposes; their characteristics are summarized in Table 1. Yarn cross section was measured by caliper, and Young Modulus was determined assuming linear elastic behavior for fibers of meshes.

Table 1: Geometrical, physical and mechanical characteristics of nets (*data provided by HARPO Spa)

	Geojuta®	***Coconet®***
Mesh size (mm)*	16x10	11.5 x 12.5
Weight (g/m^2)*	500	700
Yarn cross section (mm^2)	3.15	3.13
Tensile force (KN/m)*	15-20	20
Ultimate strain (%)*	6-8	34
Young Modulus (MPa)	785	223

Geojuta® and Coconet® reinforced six specimens showed each with either a simple configuration, i.e. net laid over the brick and plastered with earthen mortar (with composition similar to the adobe earthen but more fluid), or an anchored one consisting in the same net and mortar and steel U shaped nails ensuring a more effective fastening of the net to the adobe.

Six specimens were reinforced by Geojuta® and six by Coconet®. Two attachment systems were tested for each kind of net: the first one was made by placing the net over the brick and plastered with earthen mortar; in the second one the net was anchored to the brick by steel U shaped nails and then plastered by mortar, so ensuring a more effective fastening of the net to the adobe. In Table 2 the test plan is summarized.

Table 2: Test plan

Description	***Identification***	***Test performed***
Not reinforced adobes	ADOBE	3
Adobe + Geojuta® + earthen mortar	Jute-simple	3
Adobe + Geojuta® + U nails + earthen mortar	Jute-anchored	3
Adobe + Coconet® + earthen mortar	Coco-simple	3
Adobe + Coconet® + U nails + earthen mortar	Coco-anchored	3

3. Experimental results

The load/displacement diagrams of unreinforced, coco fiber-based reinforced and jute fiber-based reinforced specimens are reported in Figures 3, 4 and 5, respectively. The qualitative similarity of the diagrams resulted by all the tested specimens allowed the identification of average diagrams for each set of specimens. These schematic diagrams, shown in Figure 6 with the aim of comparison, are obtained using only significant points, i.e. the points that identify the end of four substantially linear branches of the load-displacement curves.

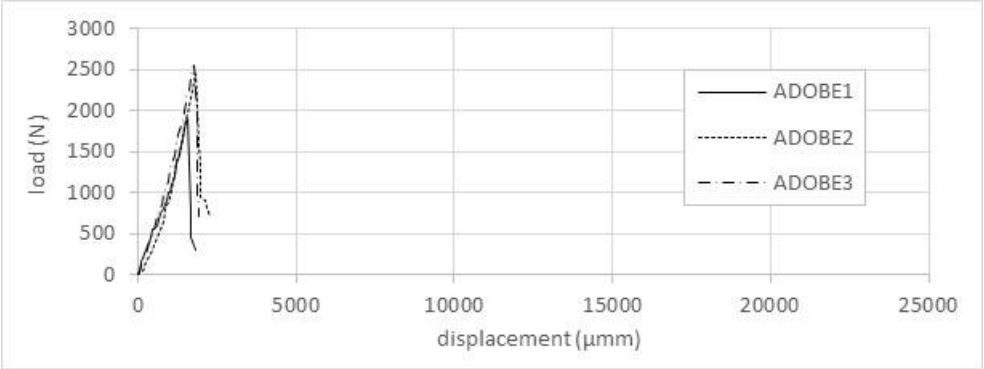

Figure 3: Load-displacement diagram of specimens without reinforcement.

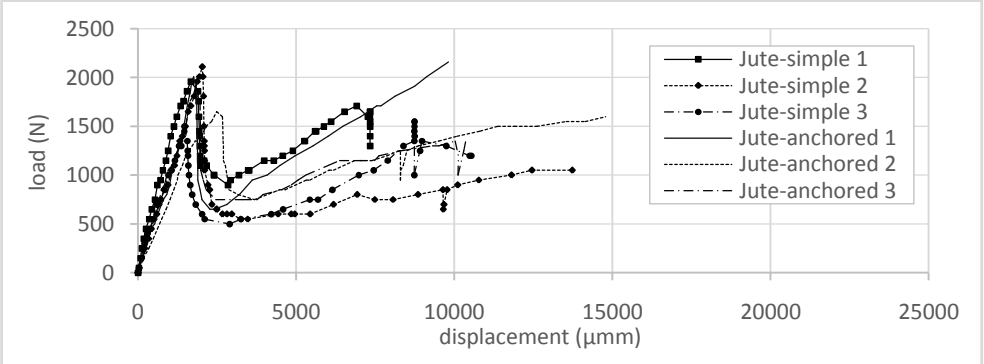

Figure 4: Load-displacement diagram specimens with of jute-based reinforcement.

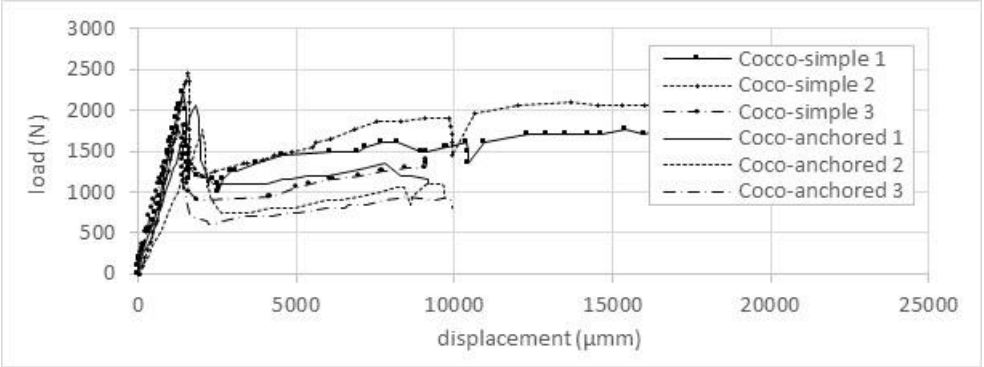

Figure 5: Load-displacement diagram specimens with of coco-based reinforcement.

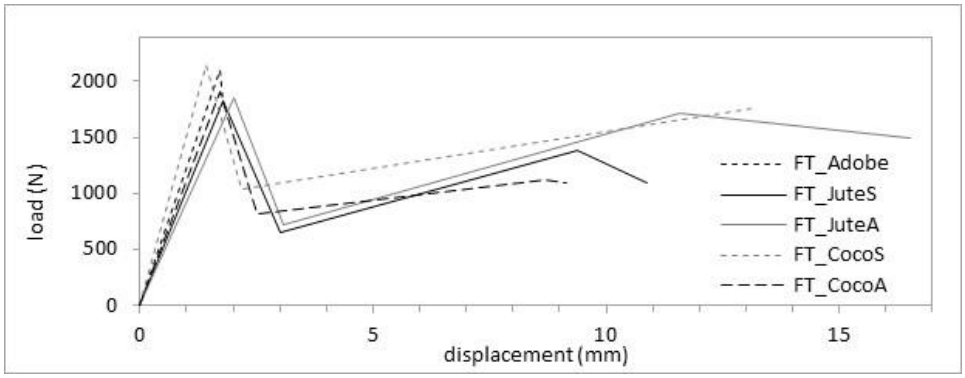

Figure 6: Schematic average diagrams.

The comparison among the diagrams shows that the fiber-based reinforcement gives a very high strain capacity. The ultimate displacements of the reinforced specimens are around 10 times greater than the ultimate displacements of the not reinforced ones. This is crucial in allowing energy dissipation under seismic actions. All the diagrams of the reinforced specimens share the same path, and two main phases can be identified: the brittle fracture of the adobe with loss of load, and the subsequent increase of load thanks to the cooperation of the net. In the first phase of the bending test, the reinforcement seems not to play any role, and no appreciable difference in the slope of the first branch of the load paths of reinforced and unreinforced specimens is recorded. The effectiveness of the reinforcement relies on the adhesion of the net to the brick. The tests show a substantial equivalence between the two types of anchorage, highlighting the ineffectiveness of the U shaped nails. The collapse mechanism always occurs for net slipping at brick interface. Figure 7 shows coco fiber-based reinforced specimens after the test.

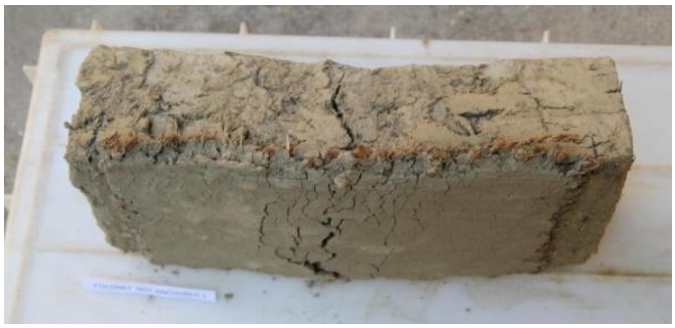

Figure 7: Coco fibre-based reinforced specimens after the test.

4. Numerical modelling

The nonlinear static analyses have been performed by means of the commercial code DIANA 9.6, (TNO Diana, 2014) and the pre and post processor embedded, Midas FX+ 3.3. Linear Elastic materials have been assumed for parts not involved in cracking phenomena, and a Total Strain fixed Crack model, which describe the tensile and compressive behavior of a material with one stress-strain relationship, or a Tresca plasticity model, for areas affected by local failure (mid span cross section of adobe and textile-matrix interface). Even if these constitutive models are not specifically designed for earthen masonry, their parameters can be calibrated to represent the salient aspects of adobe behavior in the inelastic range.

4.1. Unreinforced Adobe

Given the symmetry of geometry and load, a planar surface represents the left half of the adobe brick, and a series of 23 horizontal line elements in the x direction are placed on the symmetry axis Y, the symmetry condition constraints the x direction translations (Figure 8a).

The planar surface is meshed with 2D linear plane elements, Q8MEM, of 5 mm size, and the line elements are meshed with 1-D trusses, L2TRU, of 10 mm length. Plane elements behave linearly, and the nonlinear behavior is concentrated on trusses.

Elastic properties of plate and truss elements have been set in order to reach the same stiffness recorded in the experimental test.

Truss material follows a Total Strain Crack model with brittle tensile behavior (Fig.8d) and slight residual tensile strength after cracking, i.e. 0.02 MPa. The static nonlinear analysis representing the unreinforced condition is called UR_AdobeSYM and representative values are reported in Table 3.
The comparison between experimental and numerical load paths is showed in Figure 9.

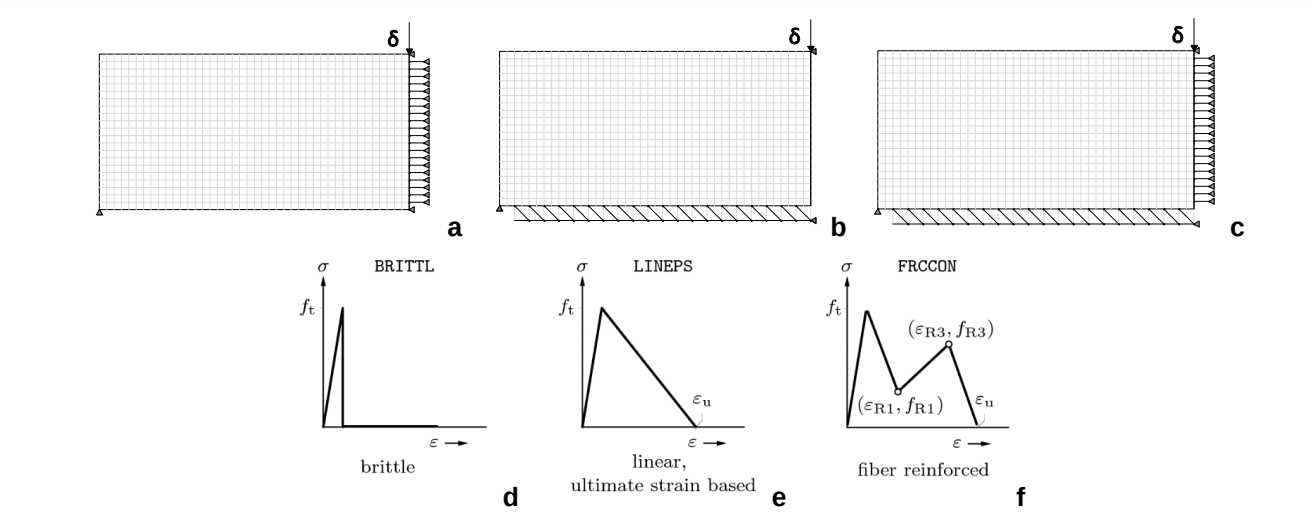

Figure 8: FEM model left half of the specimens (a, b, c); BRITTL, LINEPS and FRCCON tensile constitutive models for trusses in total strain crack model (qthelp://tnodiana.com.diana.9.6/doc/MatLib/img1335.png) (d, e, f).

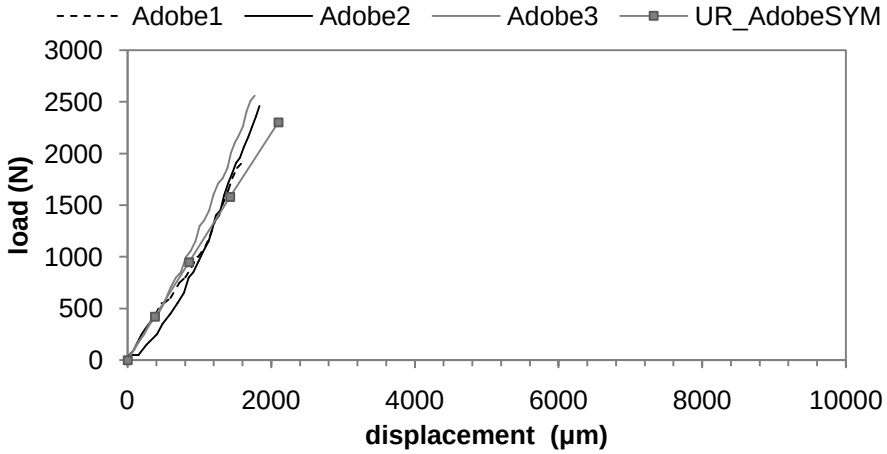

Figure 9: Unreinforced Adobe load paths.

4.2. Reinforced Adobe

The collapse configuration for all reinforced specimens showed a single fracture in the middle of the brick and any remarkable detachment of the reinforcement, Figure 7. Thus, the role played by the textile-matrix interface is dominant in the response.
The FE analyses of the reinforced configuration with jute net, applied without U-shaped nails, considers two geometrical models where the adobe part is meshed like in the unreinforced configuration. The first model considers mid span cross section completely fractured and constrained only at the edges (Figure 8b), while the other considers also the contribution offered by tensile strength of the mid span cross section, (Figure 8c) like in the model of unreinforced adobe.
The reinforcement contribution of jute or coco textile was concentrated in a truss structure hinged to the adobe brick to represent effectively the focal role of the matrix at interface between the fiber textile and the brick. The truss structure is made of a strip of eighteen squared 10x10mm modules with diagonal connections. Vertical elements are completely rigid, outer horizontal elements represent fiber textile (elastic properties defined in Tab.1) and diagonal elements work as interface. The interface behavior between textile reinforcement and the upper brick has been modeled adopting a TSCR model with different tensile behaviors for diagonal trusses; featuring parameters for each analysis are reported in Table 3.

Table 1: Tensile characteristics of FEM models (for all models the residual tensile strength for brittle or linear tensile behavior is fr = 0.02MPa)

Analysis	*Young Modulus (MPa)*	*Tensile Model*	*Tensile strength (MPa)*
UR-AdobeSYM	150	BRITTL	f_t=0.17
BT	230	BRITTL	f_t=0.36
BTLC	230	BRITTL BRITTL LINEPS FRCCON	f_{t1}=0.8 f_{t2}=0.66 f_{t3}=0.36 ε_{3u}=0.003 f_{t4}=0.36, f_{r41}=0.1; ε_{r41}=0.0321; f_{r43}=0.45; ε_{r43}=0.08; ε_{4u}=1
BTSYM	150	BRITTL	f_t =0.36
BTCSYM	230	BRITTL	f_t =0.58
BTCSYM150	150	BRITTL	ft=0.58
D_JuteSBT	230	HARDIA	f_t=0.36 ; ε_t=0.0015 ; f_{r1}=0.02 ; ε_{r1}=0.002; f_{r2}=0.03 ; ε_{r2}=0.1

BT and BTLC analyses do not consider the symmetry trusses and the Young Modulus of plate elements and diagonal truss elements have been scaled to reach sufficient stiffness. For BT analysis, a perfect brittle behavior (Figures 8d, 9b) has been considered for sloped trusses. The comparison between BT analysis load path and the experimental one shows good accordance in terms of stiffness in the linear phase, but an early loss of load caused by failure of diagonal trusses and a subsequent no stiffening phase.

To model the stiffening response of the experimental test, a combination of all the three tensile constitutive models (Figures 8d, e, f), have been adopted in analysis called BTLC. In particular, going from right to left (Figure 8b), the first four inclined trusses from symmetry axis have the highest tensile strength (ft1), the next two trusses belong to a lower tensile strength group (ft2), both these groups show brittle softening (Figure 8d and Table 3). Then, a group of nine trusses have a linear softening branch, (ft3, ε3u) (Figure 8e and Table 3) and the last three trusses next to the support follow the FRCCON behavior constitutive model (Figure 8f and Table 3). The output of this analysis shows a similar path of the experimental one. Stiffness is identical to that of the experimental load path. Failure of diagonal trusses with higher tensile strength and brittle behavior (first six trusses) occurs at nearly 90% of the value of the displacement of the experimental tests (1.59 mm instead of 1.77mm) and stiffening branch reaches the same load level, i.e. 76% of peak load.

The last analysis, BTSYM, have considered the symmetry trusses in mid span cross section and a unique tensile constitutive model, i.e. BRITTL (Figure 8d), and strength value (Table 3) for all trusses. Analyses outputs are reported in Figure 10.

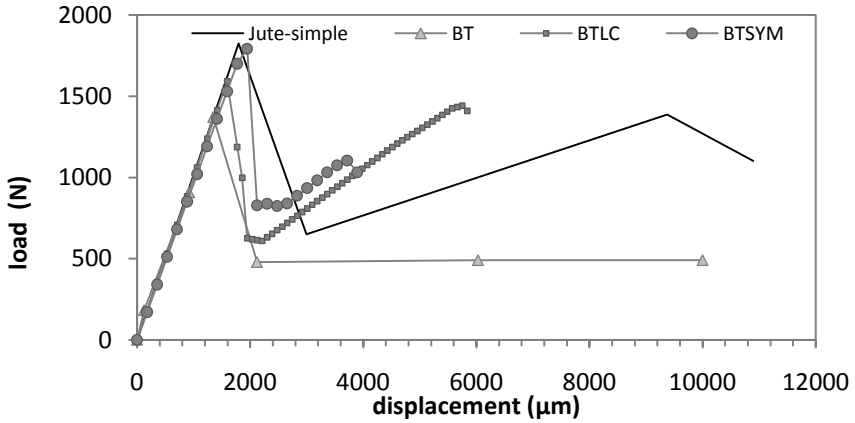

Figure 10: Experimental and numerical load paths of jute reinforced specimen.

Coco net reinforcement numerical tests have been modelled on the same geometrical basis of the model reinforced with jute net. The geometry showed in Figure 8c and the BTSYM analysis model have been

adopted. The same brittle constitutive model has been assigned to all trusses and two analyses, BTCSYM and BTCSYM150, have been performed changing only elastic modulus (Table 3). The outputs of the analyses, whose featuring load paths are reported in Figure 11, differ from results of jute reinforcement models due to a saw tooth shaped final branch. In particular, the stiffening branches show the progressive failure of trusses until final collapse. Since a pseudo stiffening behavior of the model has been reached, no further analysis was carried on.

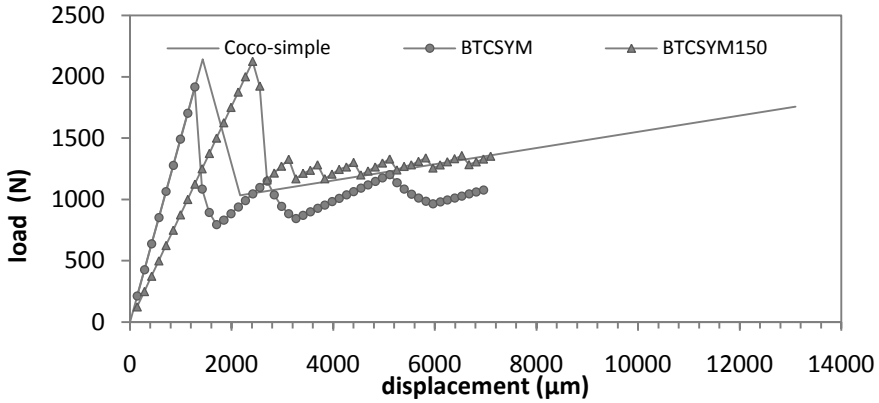

Figure 11: Experimental and numerical load paths of coco reinforced specimen.

4.3 Cyclic loading condition

A final numerical model represents a double reinforced Adobe brick subjected to cyclic loading not yet experimentally tested. The load level applied, with alternate sign, is in the dimension range of the previous tests. The cyclic load condition aims to portray the reinforcement response under seismic-like actions that alternatively invert the sign of the stress.

The model exploits an additional mirrored reinforcement on the top side of the brick and the same symmetry constraints of the previous models. The main characteristic of D_JuteSBT analysis consists in the constitutive model adopted. Instead of a TSCR model, a classical Tresca plasticity model has been adopted with a plastic strain-hardening diagram (HARDIA) defined point by point by values reported in Tab.3 and showed in Figure 12b The tensile constitutive model is similar to that of Analysis BT (Figure 8d). In particular, for the HARDIA model, the brittle behavior in tension softening has been considered as lightly linear decreasing and the residual tensile strength has been considered as slightly increasing. In Figure 12 the load displacement path and the constitutive model adopted are showed.

The sudden loss of load is caused by the actual brittle constitutive model of the stretched trusses (lower reinforcement), while the partial loss of load of trusses in the upper reinforcement is denoted by the change in the global stiffness (of the second and fourth quadrant).

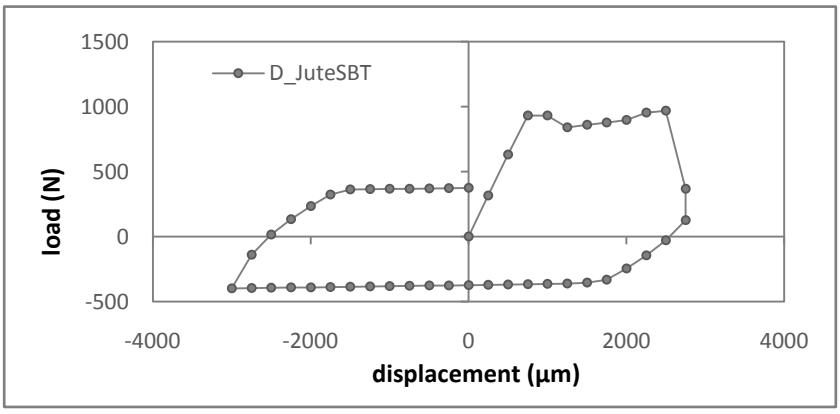

a)

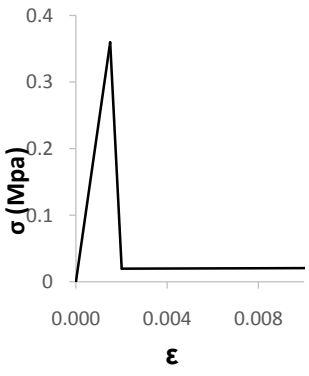

b)

Figure 12: D_JuteSBT Analysis load path a), and the slightly hardening tensile constitutive model b)

Conclusions

The numerical load paths show good agreement with experimental results. This fact encourages further investigation to deepen the comprehension of the behaviour of textile reinforcements and to develop adequate numerical tools for the reinforcement design of earthen structures.
The analysis of numerical load displacement paths suggests the following specific conclusions:

- The first geometry model (Figure 8b), which considers the specimen already fractured, has the advantage to concentrate nonlinear behaviour only in one group of elements. However, reaching an acceptable stiffening behaviour in the load path requires a cumbersome combination of different constitutive models, which is somehow not completely realistic.
- Taking in consideration the contribution of the fracture that opens at mid span cross section (geometry model of Figure 8c), permits the use of a more realistic elastic modulus for either plates and trusses and the assumption of a unique constitutive model (BTSYM analysis).
- Results of coco net reinforced specimens have showed post-peak response characterized by a saw-tooth shaped branch, differently from the jute net reinforcement. This response is caused by value of the elastic modulus of coco net lower than jute net.
- The simulation of a cyclic loading condition has needed a different constitutive model in order to simulate a permanent deformation in the unloading phase. Further investigation on this topic will regard future research.

Acknowledgments

The authors wish to thank Flavio Ridolfi and Dalia Omar Sidick for their helpful collaboration during the tests activities within the development of their doctoral thesis.
SEIC Geotecnica of Harpo Spa (Trieste, Italy) is gratefully acknowledged for the supply of the textiles used in this research.

References

1. Baglioni E., Mecca, S., Rovero, L., Tonietti, U., Traditional Building Techniques of the Drâa Valley (Morocco), *DIGITAR*, 1, (2013), 79-87, ISSN:2182-844X.
2. Blondet M., Villa García G., Loaiza C., ¿Viviendas sismorresistentes de tierra? Una visión a Futuro, *XIV Congreso Nacional de Ingeniería Civil*, (2003), Perú: Colegio de Ingenieros del Perú.
3. Blondet M., Aguilar, R., Seismic protection of earthen buildings. Conferencia Internacional en Ingenieria Sismica, (2007), Lima, Perù.
4. Briccoli Bati S., Rovero L., Tonietti U., Experimental analysis for the compressive strength evaluation of the Earth Material, *Terra 2008: 10TH International Conference on the Study and Conservation of Earthen Architectural Heritage*, (2008), Bamaco, Mali, 2008.
5. Briccoli Bati S., Rovero L., Towards a methodology for estimating strength and collapse mechanism in masonry arches strengthened with Fibre Reinforced Polymer applied on external surfaces, *Materials and Structures*, 41 (7), (2008), 1291-1306.
6. Fischer A., Manual de construcciones sismorresistentes en adobe, tecnología de geomalla. *Perú: Cooperación Alemana al Desarrollo*, (2009), GTZ. 66, 7-8.
7. Fratini F., Pecchioni, E., Rovero, L., Tonietti, U., The earth in the architecture of the historical centre of Lamezia Terme (Italy): Characterization for restoration, *Applied clay science*, 53 (3), (2011), 509-516.
8. Gamrani N., Chaham K. R., Ibnoussina M., Fratini, F., Rovero, L., Tonietti, U., Mansori, M., Daoudi, L., Favotto, C., Youbi N., The particular ‘‘rammed earth’’ of the Saadian sugar refinery of Chichaoua (XVIth century, Morocco): mineralogical, chemical and mechanical characteristics, *Environmental Earth Sciences*, 66 (1) (2012), 129-140.
9. Hardy M., Cancino C., Ostergren, G., Proceedings of the Getty Seismic Adobe Project 2006 Colloquium, *The Getty Conservation Institute*, (2006), Los Angeles.
10. Houben H., Guillaud H., Earth construction. A comprehensive guide, *CRATerre-EAG*, (2005), ITDG Publishing, Bourton.
11. Islam M.S., Iwashita, K., Earthquake resistance of adobe reinforced by low cost traditional materials, *Journal of Natural Disaster Science*, 32, (2010), 1-21.

12. Méndez M.T., Vásquez, G., Corasao, I., y otros., Prototipo de Comunidad Saludable para áreas rurales del Perú: distrito de Chincha Baja, Ica. *Libro de Ponencias del Congreso TERRA BRASIL 2008*, (2008), Anais, Sao Luis de Marañao. Brasil.
13. Méndez M. T. et al., Malla de junco como refuerzo para construcciones en adobe, *Centro de Estudios para Comunidades Saludables*, (2010), Universidad Ricardo Palma, Lima.
14. Minke G., Construction manual for earthquake-resistant houses built with earth, *University of Kassel*, (2001), Kassel.
15. Morel J.C., Pkla, A., A model to measure compressive strength of compressed earth blocks with the "3 points bending test", *Construction and Building Materials*, 16, (2002), 303-310.
16. Omar Sidik D., Ridolfi, F., Rovero, L., Tonietti, U., Experimental Investigation on the anti-seismic effectiveness of textile-fibres net applied on earthen buildings. *Int. Conf. on Earthen Architecture in Asia*, (2011), Mokpo, Republic of Korea.
17. Omar Sidik D., Ridolfi, F., Rovero, L., Tonietti, U, Earthen Costruction and Seismic Risk, Reincontre internationale sur le patrimonie architectural méditerranéen 4, (2011), M'Sila – Algérie, April 10-12, 1-10.
18. Joint Australia/New Zealand Technical Committee, NZS 4298 (1998): Materials and workmanship for earth buildings. Materials and workmanship for earth buildings, *Standards New Zealand*, (1998), Wellington.
19. Rotunno T., Rovero, L., Tonietti, U., Briccoli Bati, S., Experimental Study of Bond Behavior of CFRP-to-Brick Joints, *Journal of Composites for Construction*, 19 (3) (2015), 1-14.
20. Rovero L., Focacci, F., Stipo, G., Structural behavior of arch models strengthened using FRP strips of different lengths, *Journal of Composites for Construction*, 17, (2013), 249-258.
21. Rovero L., Tonietti, U., Fratini, F., Rescic, S., The salt architecture in Siwa oasis – Egypt (XII–XX centuries), *Construction and Building Materials*, 23 (7), (2009), 2492-2503.
22. Rovero L., Fratini, F., The Medina of Chefchaouen (Morocco): A survey on morphological and mechanical features of the masonries, *Construction and Building Materials*, 47, (2013), 465-479.
23. Rovero L., Tonietti, U., Structural behavior of earthen corbelled domes in the Aleppo's region, *Materials and Structures*, 45, (2012), 171–184.
24. Rovero L., Tonietti, U., A modified corbelling theory for domes with horizontal layers, *Construction and Building Materials*, 50, (2014), 50-61.
25. Sani F., Moratti, G., Coli, M., Laureano, P., Rovero, L., Tonietti, U., Coli, N., Integrated geological-architectural pilot study of the Biet Gabriel-Rufael rock hewn church in Lalibela, northern Ethiopia, Italian Journal of Geosciences, 131 (2), (2012), 171-186.
26. Torrealva, D., Cerròn,C., Espinoza, Y., Shear and out-of-plane bending strength of adobe walls externally reinforced with polypropylene grids, *Proceeding of the XIV World Conference of Earthquake Engineering*, (2008), Beijing, China.
27. Vargas J., Torrealva, D., Blondet, M., Manual: Construcción de casas saludables y sismo resistentes de adobe reforzado con geomalla. *PUCP*, (2007), Lima.
28. Walker P., Standards Australia, Standards Australia Handbook 195. The Australian earth building handbook. *Standards Australia International Ltd*, (2002), Sydney.
29. TNO DIANA BV, DIANA - Finite Element Analysis User's Manual release 9.6, *TNO Diana BV*, (2014), Delft.